Bioconjugate Chemistry

Article

pubs.acs.org/bc

Metallization of Double-Stranded DNA Triggered by Bound Galactose-Modified Naphthalene Diimide

Kohei Komizo,[†] Hideyuki Ikedo,[†] Shinobu Sato,[†,‡] and Shigeori Takenaka*[,†,‡]

[†]Department of Applied Chemistry and [‡]Research Center for Biomicrosensing Technology, Kyushu Institute of Technology, 1-1 Sensui-cho, Tobata-ku, Kitakyushu, Fukuoka 804-8550, Japan

Supporting Information

ABSTRACT: Naphthalene diimide (NDI) derivatives bearing galactose moieties through different spacers, NDI-DS1 and NDI-DS2, were synthesized by the click reaction of the acetylene derivatives of NDI with galactose azide. They bound to double-stranded DNA with threading intercalation, as confirmed by the topoisomerase I assay and circular dichroism spectroscopy. The binding affinities of these ligands were on the order of 10^5 M^{-1} with several-fold higher affinity for double-stranded DNA than for single-stranded DNA. The silver mirror reaction on the double-stranded DNA bound to these ligands afforded silver nanowires that were converted to gold nanowires. In the atomic force microscopy measurements, the increased height of DNA areas on a mica plate was observed in the case of double-stranded DNA after NDI-DS2 treatment and subsequently silver mirror reaction, whereas the increased height of DNA areas was not observed in the case of single-stranded DNA after the same treatment.

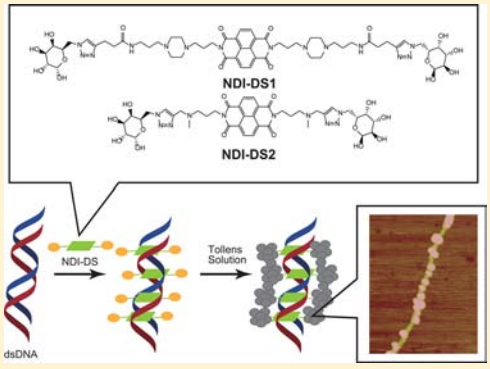

INTRODUCTION

Recently, further densified integration has been required in semiconductive devices; many nanodevices have been constructed for this purpose. Although top-down and bottom-up approaches are used to fabricate nanodevices, the latter approach is mainly used for molecular wires using carbon nanotubes,[1] conducting polymers,[2] and metal nanowires.[3] However, it is difficult to arrange these materials in the desired manner. DNA can be assumed to be a linear polymer with a diameter of 2 nm, and a branched wire can be formed by creating a DNA sequence. Furthermore, DNA can be replicated using molecular biology approaches. Therefore, many studies have focused on the nanowires of DNA.[4] As part of these studies, designed structures have been investigated using DNA complementarity, pioneered by Seeman,[5] and developed as DNA origami by Rothemund.[6] This technique is used to construct not only two-dimensional structures such as honeycombs[7] and tiles[8] but also three-dimensional structures such as cubic structures.[9] Although the DNA structure is not stable and exhibits poor conductivity, structured DNA has been utilized as the template for metallization.[10−12] DNA template metallization has been conducted by three methods: metallization of metal ions concentrated on DNA through electrostatic or coordinate interactions,[10] metallization of metal nanoparticles introduced on DNA,[11] and metallization of metal ions through modified DNA by reductive function.[12]

Herein, we synthesized threading intercalators bearing galactose moieties as the reducing sugar to introduce a reductive functionality into DNA indirectly, affording DNA template metal nanowires. Figure 1 shows the concept of DNA template metallization using naphthalene diimides (NDIs) bearing galactose moieties, NDI-DS1 and NDI-DS2, with different linker chain lengths. NDI acts as a threading intercalator, forming a stable complex with double-stranded DNA bearing many intercalators at every second base pair under saturated binding conditions.[13] After the silver mirror reaction of this complex, the silver ions were reduced by the galactose moieties of the ligands bound to double-stranded DNA, and silver metal was precipitated along the entire length of the DNA.

In this paper, we report the synthesis and binding affinity of NDI-DS1 and NDI-DS2 with DNA and the preparation of nanowires using DNA coated with NDI-DS1 or NDI-DS2. This metallization occurred only on the double-stranded region of DNA, indicating its preference for double-stranded DNA over single-stranded DNA.

RESULTS AND DISCUSSION

Mode of Interaction of NDI-DS1 or NDI-DS2 with Double-Stranded DNA. NDI-DS1 and NDI-DS2 were synthesized by the route shown in Figure 2. The absorbance maximum of 5.0 μM NDI-DS1 in 10 mM MES buffer and 1.0 mM EDTA (pH 6.25) containing 100 mM NaCl at 384 nm shows a hypochromic effect (57%) and a red shift (2 nm) upon the addition of calf thymus DNA (CT-DNA) (Figure 3A). The solution of 80 μM CT-DNA in 10 mM MES buffer and 1.0 mM

Received: June 12, 2014
Revised: July 7, 2014
Published: July 11, 2014

   dx.doi.org/10.1021/bc500263b | Bioconjugate Chem. 2014, 25, 1547−1555

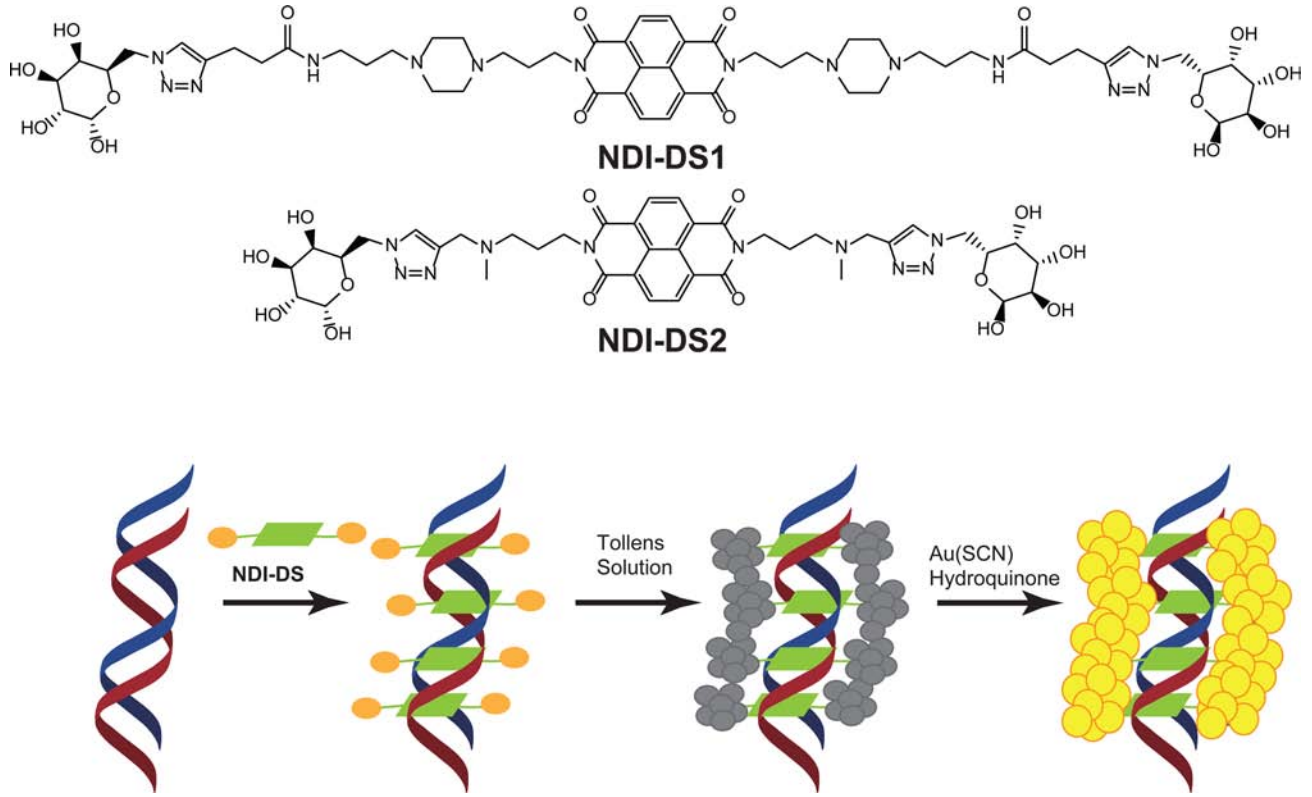

Figure 1. Chemical structures of NDI-DS1 and NDI-DS2 and DNA metallization based on their noncovalent interaction with double-stranded DNA.

EDTA (pH 6.25) containing 100 mM NaCl showed a negatively induced CD band at 383 nm upon the addition of NDI-DS1 (Figure 3B). The topoisomerase I assay conducted by addition of 1−20 μM NDI-DS1 to 0.5 μg of pBR322 shows the unwinding of supercoiled plasmid DNA by atomic force microscopy (AFM) (Figure 1S of the Supporting Information). The viscometric titration of NDI-DS1 with $[poly(dA\text{-}dT)]_2$ shows the intercalation binding of NDI-DS1 for double-stranded DNA (Figure 2S of the Supporting Information). All the data obtained here show that NDI-DS1 binds to double-stranded DNA via an intercalation mode, particularly threading, the one expected with its chemical structure.[13] Because similar characteristics were observed in the case of NDI-DS2 in these experiments (Figures 3S and 4S of the Supporting Information), NDI-DS2 also binds to the double-stranded DNA via a threading intercalation mode.

Binding Analysis of NDI-DS1 and NDI-DS2 with Double-Stranded DNA. The absorption change in 5.0 μM NDI-DS1 or NDI-DS2 in 10 mM MES buffer and 1.0 mM EDTA (pH 6.25) containing 100 mM NaCl at 384 nm upon the addition of CT-DNA (Figure 3A and Figure 3SA of the Supporting Information) was monitored, and the binding constant and binding site size were estimated by fitting the theoretical curve (Figure 5S of the Supporting Information and Table 1).[13] The binding constants of NDI-DS1 and NDI-DS2 were 3.5×10^5 and 6.8×10^5 M^{-1}, respectively, with a similar binding site size of 2.3, consistent with disubstituted NDI derivatives.[13] The binding site size of ∼2 is based on the nearest-neighbor excluded site model,[13] and these ligands can bind to double-stranded DNA every 2 bp. The binding preference of NDI-DS1 was evaluated by measuring the binding constants for AT and GC DNA using SPR experiments (Figure 6S and Table 1S of the Supporting Information); we found an approximately 3-fold higher affinity of NDI-DS1 for GC DNA than for AT DNA.

The association or dissociation rate constants of NDI-DS1 and NDI-DS2 for CT-DNA were estimated using a stopped-flow spectrophotometer by fitting the time traces of absorbance at 383 nm (Figure 7S of the Supporting Information). The SDS-driven dissociation rate constants of NDI-DS1 or NDI-DS2 for CT-DNA were measured by mixing the SDS solution with the NDI-DS1 or NDI-DS2 solution containing CT-DNA. The association rate constants of NDI-DS1 and NDI-DS2 with CT-DNA were 1.2×10^4 and 4.7×10^4 M^{-1} s^{-1} with dissociation rate constants of 0.13 and 0.21 s^{-1}, respectively (Table 1). NDI-DS1 and NDI-DS2 exhibited a relatively strong binding affinity on the order of 10^5 M^{-1} for double-stranded DNA with slow dissociation rate constants, similar to that expect for a threading intercalator. In a close comparison of these ligands, NDI-DS2 shows a binding affinity 2-fold higher than that of NDI-DS1, because its association rate is faster than that of NDI-DS1.

To estimate the preference of ligands for double-stranded DNA over single-stranded DNA, the binding affinity of these ligands was estimated using 8-mer oligonucleotides, ds-ODN or ss-ODN. ds-ODN was a self-complementary oligonucleotide and used after annealing as its double-stranded form at 25 °C [T_m = 51 °C; 10 mM Tris-HCl (pH 7.4), 1.0 mM EDTA, and 150 mM NaCl (Figure 8S of the Supporting Information)]. Spectrophotometric titration of these ligands with ds-ODN or ss-ODN and their Benesi−Hildebrand plot analysis afforded their binding affinity as 10^5 M^{-1} order of *nK*. NDI-DS1 or NDI-DS2 showed a 2- or 5-fold higher affinity for ds-ODN than for ss-ODN, respectively.

dx.doi.org/10.1021/bc500263b | *Bioconjugate Chem.* 2014, 25, 1547−1555

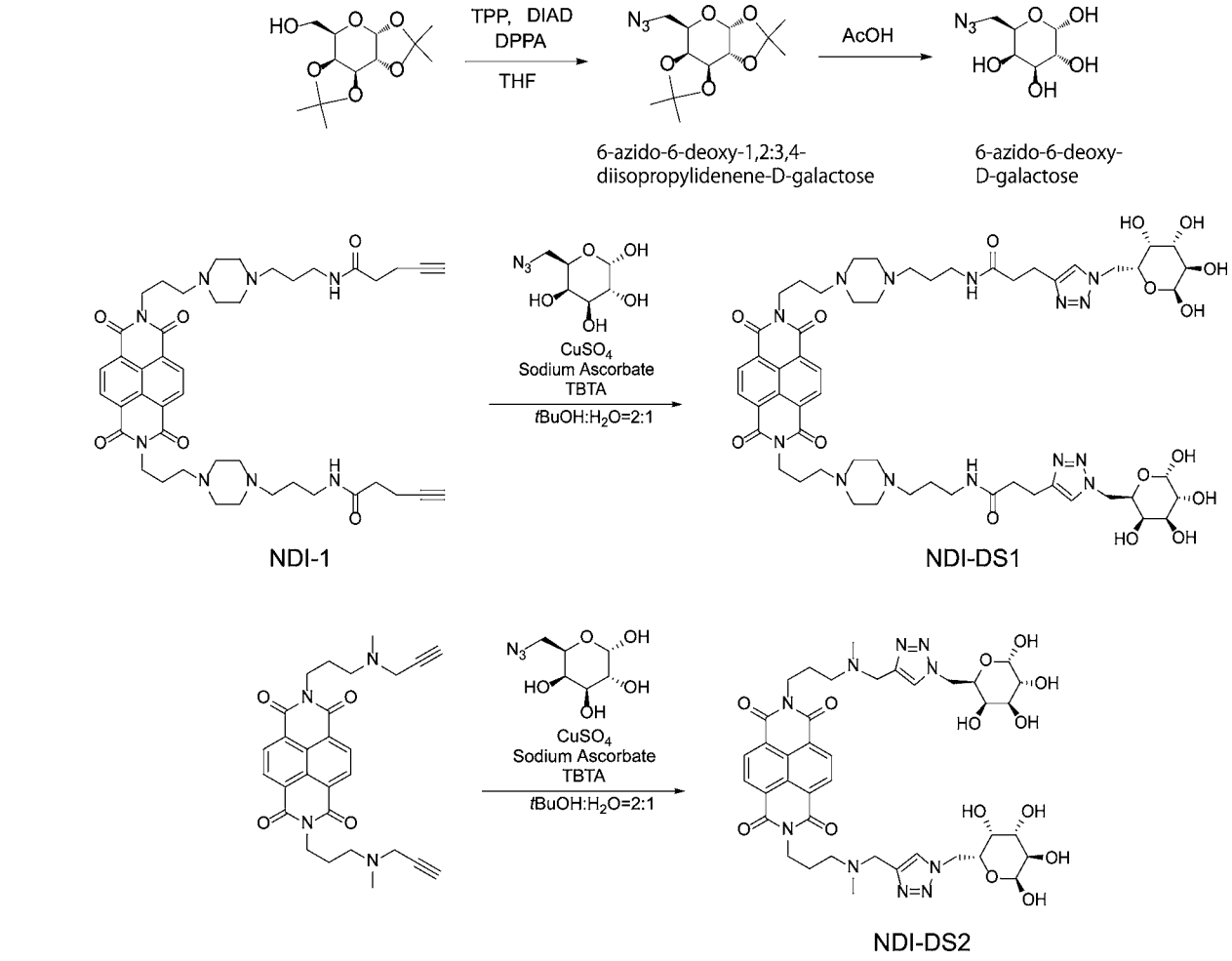

Figure 2. Synthetic route of NDI-DS1 and NDI-DS.

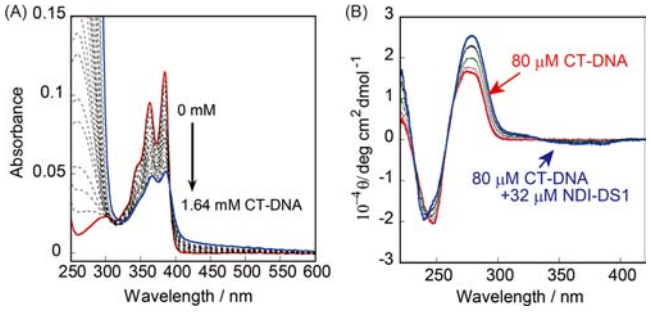

Figure 3. (A) Absorption change of 5.0 μM NDI-DS1 upon addition of CT-DNA. (B) Circular dichroism spectral change of 80 μM CT-DNA upon addition of NDI-DS1 in 10 mM MES buffer and 1.0 mM EDTA (pH 6.25) containing 100 mM NaCl.

Table 1. Binding Parameters of NDI-DS1 and NDI-DS2 with CT-DNA, ds-ODN, or ss-ODN

DNA		NDI-DS1	NDI-DS2
CT-DNA[a]	K/M^{-1} (n)	3.5×10^5 (2.3)	6.8×10^5 (2.3)
	$k_a/M^{-1}s^{-1}$	1.2×10^4	4.7×10^4
	k_d/s^{-1}	0.13	0.21
ss-ODN[b]	nK/M^{-1}	1.5×10^5	1.7×10^5
ds-ODN[b]	nK/M^{-1}	3.3×10^5	1.0×10^6

[a]Scatchard plot. [b]Benesi–Hildebrand plot.

Silver Mirror Reaction of NDI-DS1 or NDI-DS2. First, we checked whether NDI-DS1 and NDI-DS2 can reduce silver as described by the following equation:

$$\text{R-CHO} + 2[\text{Ag}(\text{NH}_3)_2]^+ + 2\text{OH}^- \rightarrow \text{R-COOH} + 2\text{Ag} + 4\text{NH}_3 + \text{H}_2\text{O}$$

Two microliters of 0.1 M $Ag(NH_3)_2$, prepared by the addition of NH_3 to 0.1 M $AgNO_3$, was placed on four spots on a glass plate, and a solution of 11 mM glucose, NDI-1, NDI-DS1, or NDI-DS2 containing 0.26 M NaOH was placed on these spots, where NDI-1 is naphthalene diimide without galactose moieties as the negative control. Silver precipitation was observed in the case of glucose and NDI-DS1, indicating that NDI-DS1 and NDI-DS2 can participate in the silver mirror reaction.

Second, the DNA–NDI-DS1 complex was observed by AFM. Panels A and B of Figure 4 show the AFM image of linearized M13 DNA in the absence or presence of NDI-DS1. The DNA lengths, estimated by ImageJ, changed from 2013 ± 134 to 2074 ± 218 nm after NDI-DS1 binding. The average increase in the chain length of DNA by NDI-DS1 binding was 61 nm. This behavior is consistent with the DNA length increasing upon intercalation and unwinding of the intercalator, as monitored by AFM.[14] The silver mirror reaction was conducted for the complex, M13–NDI-DS1, on the plate for 5 h. Nanoparticles (20–50 nm) were observed along the entire

dx.doi.org/10.1021/bc500263b | Bioconjugate Chem. 2014, 25, 1547–1555

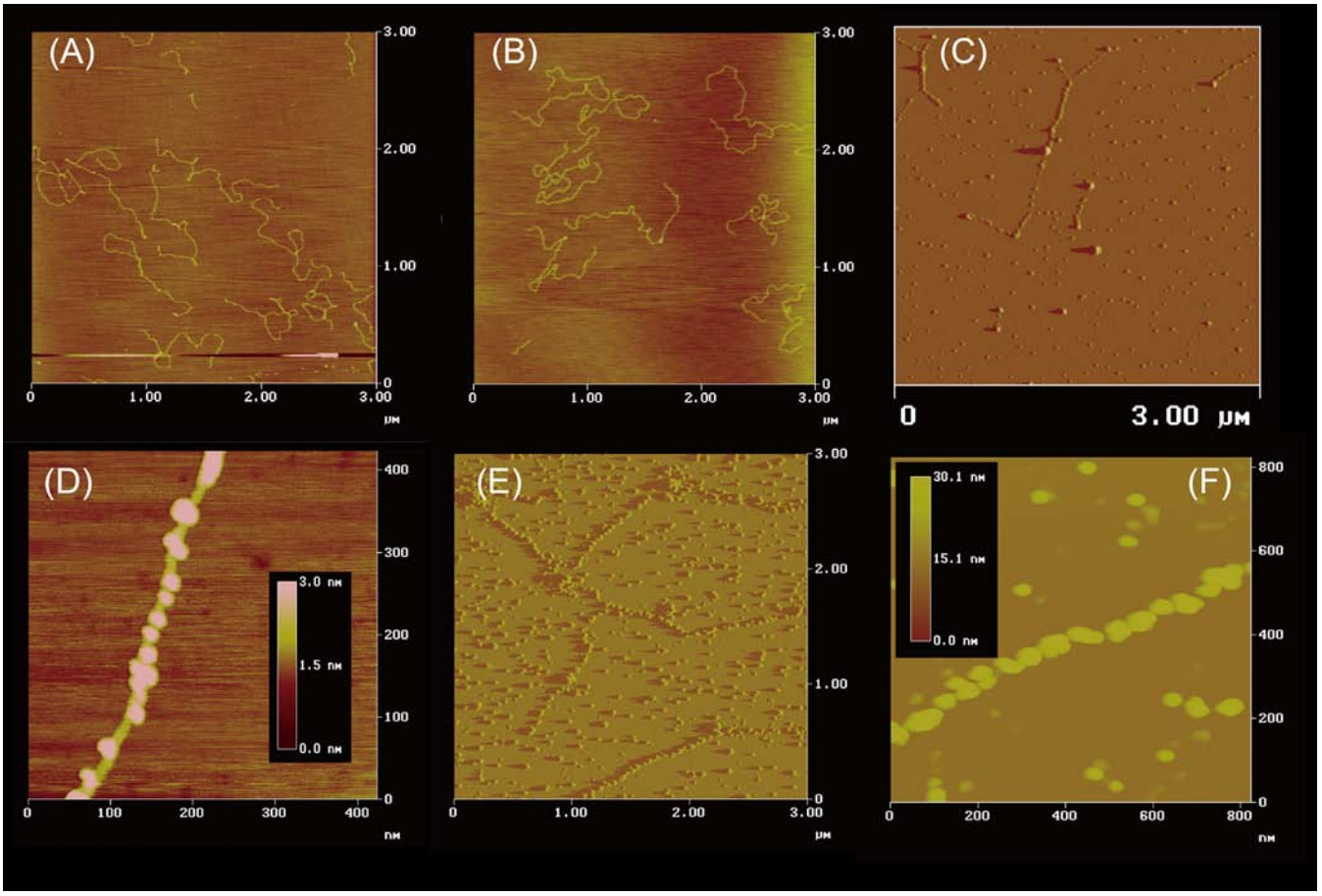

Figure 4. Atomic force microscopy images of linearized M13 DNA: (A) 0.16 ng/μL M13, (B) 0.16 ng/μL M13 and 400 nM NDI-DS1, and (C) 0.16 ng/μL M13 and 400 nM NDI-DS1 after treatment with 0.1 M $AgNO_3$ and NH_3. (D) Extended image of the section in panel C. (E) Image of 0.50 ng/μL λDNA and 2250 nM NDI-DS1 after treatment with 0.1 M $AgNO_3$ and NH_3 and subsequent treatment with 60 mg/mL KSCN and 23 mg/mL $KAuCl_4$ in phosphate buffer (pH 5.5). (F) Extended image of the section in panel E.

length of DNA, as shown in panels C and D of Figure 4. Because the transmission electron microscopy (TEM) measurement showed that these particles were composed of silver, we can conclude that we successfully prepared DNA template silver nanowires (Figure 5). The height of M13 DNA increased from 0.6 to 2.0 nm after the silver mirror reaction. The silver atoms may have originated from the galactose core of NDI-DS1 bound to DNA. Because silver ion has a diameter of 0.25 nm, four or five atoms of silver accumulated in this case. The height of DNA did not change at a longer reaction time of 18 h (Figure 9S of the Supporting Information). Nanoparticles unconnected along DNA were observed in panels C and D of Figure 4. This behavior was similar to that at higher NDI-DS1 concentrations (Figure 10S of the Supporting Information). Because NDI-DS1 has a slight preference for the GC-rich sequence as shown in Table 1, the heterogeneity of the nanoparticles on DNA should arise from the heterogeneity of NDI-DS1 binding on the DNA sequence.

Furthermore, the reduction of gold ion was conducted on the silver nanowires on DNA using λDNA with a longer length because shorter M13 DNA easily peeled off after the metallization by silver. Chloroauric acid and KSCN were used to reduce gold on the silver nanowires of DNA after the hydroquinone treatment according to the following equation:

$$AuCl_4^- + 4SCN^- \rightarrow Au(SCN)_2^- + (SCN)_2 + 4Cl^-$$

The silver nanowires became covered with gold after the reduction of $Au(SCN)_2^-$ near the silver nanoparticles. Subsequently, nanoparticles with a height of ~23 nm were observed after a 30 s treatment, as shown in panels E and F of Figure 4. A 60 s treatment afforded a DNA with a height of 46 nm, indicating that the size of nanowires can be controlled by varying the reaction time (Figure 11S of the Supporting Information). The scattering of nanoparticles is based on the nonspecific adsorption of NDI-DS1 on the plate through silver nanoparticles. This arises from the poor washing of the plate because of the easy removal of silver-metallized DNA. The formation of gold nanoparticles was not observed for the untreated DNA complex with NDI-DS1 or DNA alone (Figure 12S of the Supporting Information). These results indicate that the DNA nanowires were formed by the complexation of NDI-DS1 with double-stranded DNA.

Figure 5 shows the results of TEM (A and B) and energy-dispersive X-ray spectroscopy (EDS) (C) measurements of gold nanowires prepared by the silver mirror reaction of M13 bound to NDI-DS1. Nanoparticles (~20 nm) were observed, as shown in panels A and B of Figure 5, and these nanowires consisted of silver, as identified by EDS measurements (Figure 5C). Figure 5A shows the branching structure along the length of DNA, and this may have resulted from the remaining NDI-DS1 near the DNA. Such a branching structure has been

dx.doi.org/10.1021/bc500263b | Bioconjugate Chem. 2014, 25, 1547−1555

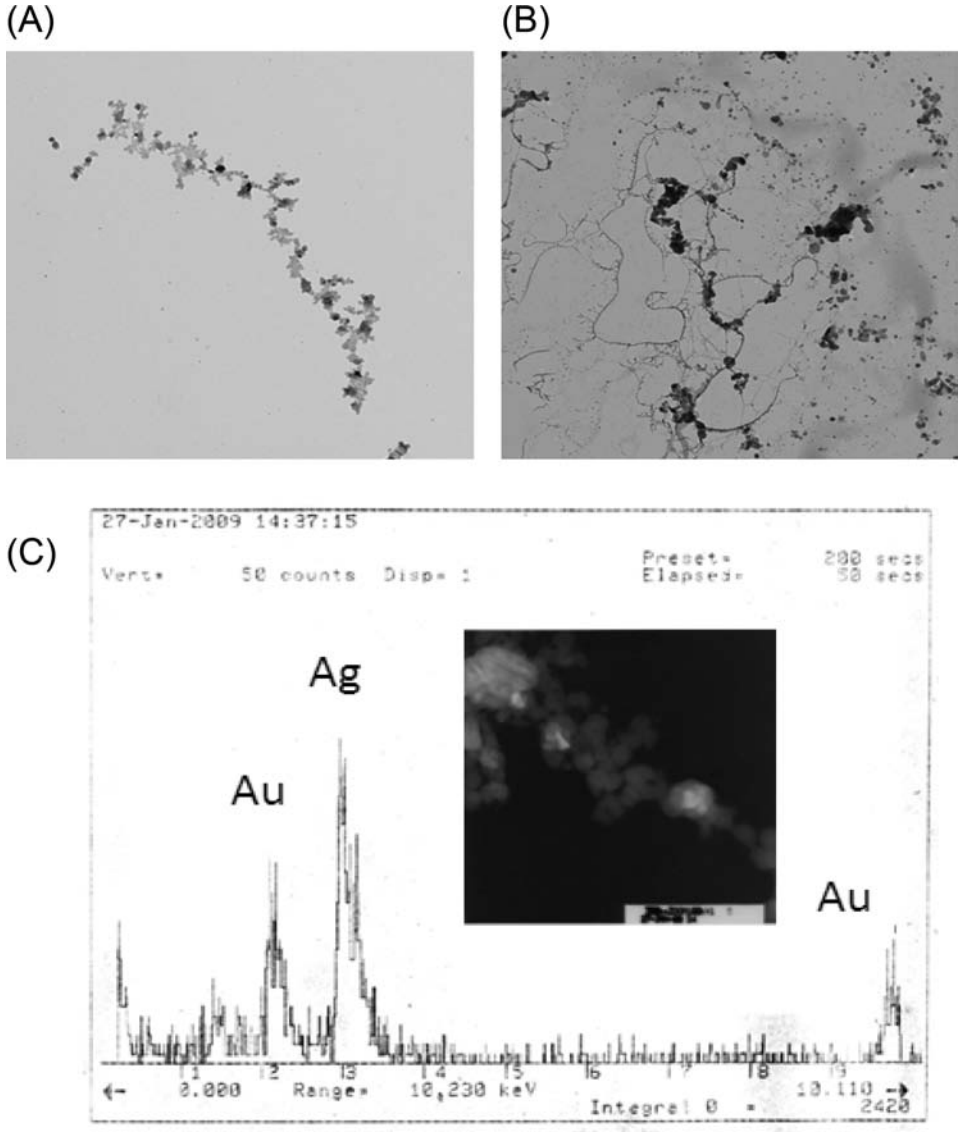

Figure 5. (A) Transmission electron microscopy image of the complex between 0.001 ng/μL M13 and 1.5 nM NDI-DS1 on the Au plate after treatment with 0.1 M $AgNO_3$ containing NH_3. (B) Extended image of the section in panel A. (C) Energy-dispersive X-ray spectroscopy measurement of the particle site of panel A.

reported in the case of DNA template Pd nanowires by Richter.[15]

Finally, silver metallization using NDI-DS2 was conducted in the case of single-stranded M13 DNA (ssDNA) and double-stranded M13 DNA (dsDNA) (Figure 6A). The AFM images of ssDNA and dsDNA showed heights of ~0.25 and 0.5 nm, respectively. These values are reasonable because single- and double-stranded DNAs were observed in the AFM image. The AFM image of the mixture between 2.0 ng/μL dsDNA and 6.7 μM NDI-DS2 (1:1 DNA-bp:NDI-DS) showed the unwinding of circular M13 plasmid DNA, whereas the mixture between 2.0 ng/μL ssDNA and 6.7 μM NDI-DS2 (1:1 DNA-b:NDI-DS) showed an aggregated complex. The heights of these complexes for dsDNA and ssDNA were 0.4 and 0.25 nm, respectively. After the silver mirror reaction, an increased height of 0.9 nm was observed in the case of dsDNA, whereas no change in height was observed in the case of ssDNA (0.4 nm) (Figure 6B). This result indicates that silver metallization occurred in the case of double-stranded DNA bound to NDI-DS2 effectively.

Upon comparison of the metallization using NDI-DS1 and NDI-DS2, sliver nanoparticles of ~1 nm were observed in the case of NDI-DS2, smaller than that observed in the case of NDI-DS1 (2 nm). This result indicates that NDI-DS2 utilized the metallization of double-stranded DNA specifically. The difference in the height of nanowires can be attributed to a difference in the linker length of NDI-DS1 and NDI-DS2: A shorter linker chain length of NDI-DS2 placed galactose moieties in the groove of double-stranded DNA, whereas the galactose of NDI-DS1 stepped out from the DNA groove.

■ CONCLUSION

NDI-DS1 and NDI-DS2 bearing galactose moieties were synthesized as the metallization reagents for double-stranded DNA by the reduction of silver ions. These ligands bound to double-stranded DNA with threading intercalation to cover the galactose moieties with DNA, thus affording silver or gold nanowires using DNA as the template. Compared to other previous reports on DNA template metallization, this system achieved the selective metallization of double-stranded DNA. It

dx.doi.org/10.1021/bc500263b | *Bioconjugate Chem.* 2014, 25, 1547−1555

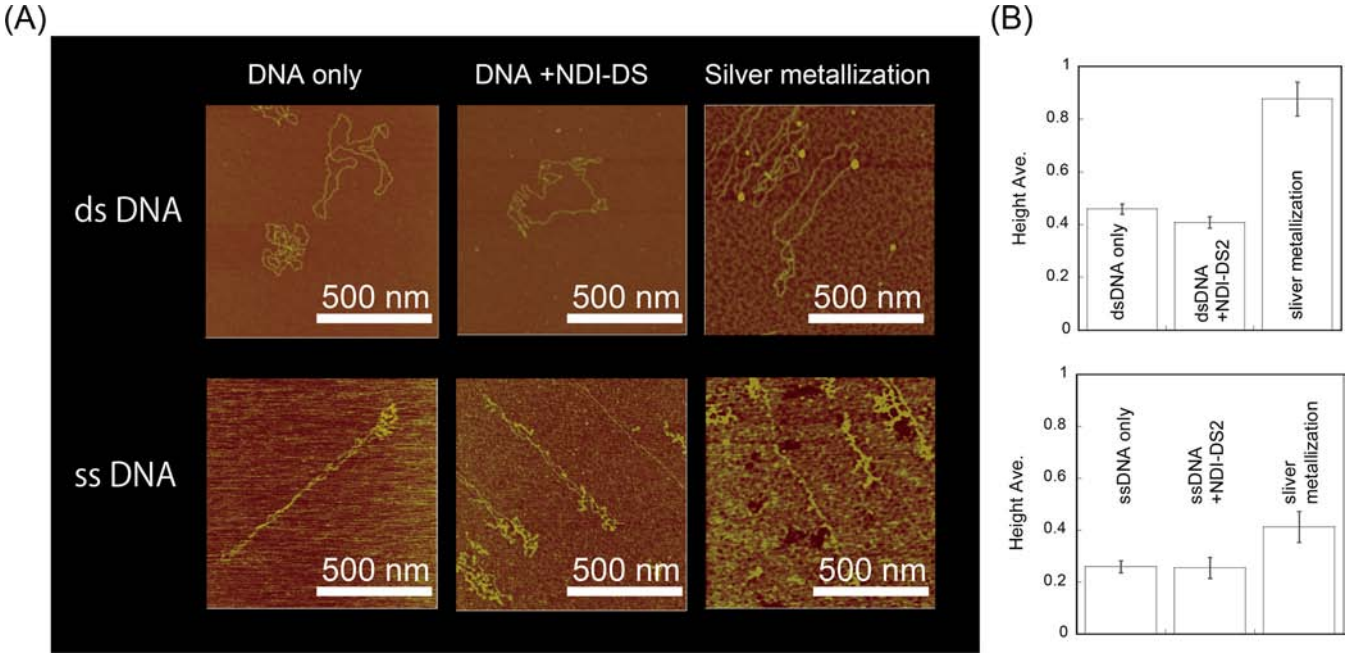

Figure 6. (A) AFM imaging of double- and single-stranded DNA before and after treatment with NDI-DS2 and subsequently sliver metallization. (B) DNA heights at each step.

is interesting to remove organic components from the obtained nanowire after burning. This is underway in our laboratory. This is useful for the synthesis of metal nanowires bearing single-stranded DNA as the sticky ends for further applications, which should assemble the obtained nanowires through hybridization with their complementary strand.

EXPERIMENTAL SECTION

Materials. 2-Morpholinoethanesulfonic acid monohydrate (MES) and ethylenediamine-*N*,*N*,*N*′,*N*′-tetraacetic acid tetrasodium salt tetrahydrate (EDTA) were purchased from Dojindo (Kumamoto, Japan). M13mp18 single-stranded DNA (Virion DNA), pBR322, topoisomerase I, and *Eco*RI were purchased from Takara Bio (Shiga, Japan). CT-DNA was purchased from Sigma-Aldrich (St. Louis, MO) and used after fragmentation.[16] Oligonucleotides, 5′-GCACGTGC-3′ and 5′-GCTCGGCA-3′, which are different in a DNA sequence with same base content, were custom synthesized by Genenet (Fukuoka, Japan). Self-complementary 5′-GCACGTGC-3′ was used as the double-stranded oligodinucleotide (ds-ODN) after annealing, and 5′-GCTCGGCA-3′ was used as the single-stranded oligodinucleotide (ss-ODN). The reagents were purchased from Tokyo Chemical Industry Co. Ltd. (Tokyo, Japan).

Synthesis of 6-Azido-6-deoxy-1,2:3,4-diisopropylidene-D-galactose. Azido galactose was synthesized as follows according to a procedure described previously.[17] 2,2′-Azodi(2-methylbutyronitrile) (DIAD, 3.7 g, 14 mmol) and triphenylphosphine (Ph_3P, 3.8 g, 14 mmol) were added to a solution of 1,2:3,4-diisopropylidene-D-galactose (3.7 g, 14 mmol) in 30 mL of tetrahydrofuran at 0 °C, and the mixture was stirred for 15 min. After the addition of diphenylphosphoryl azide (DPPA, 3.0 mL, 14 mmol), the reaction mixture was stirred overnight. Furthermore, DIAD (2.9 g, 149 mmol) and Ph_3P (3.8 g, 148 mmol) were added, and the mixture was stirred for 15 min; next, DPPA (3.1 mL, 148 mmol) was added and the mixture stirred for 2 days. The reaction mixture was chromatographed, and the fraction at R_f = 0.39 (developing solvent, CH_2Cl_2) was collected to afford 2.2 g (56% yield) of azido galactose as a colorless viscous oil after evaporation under reduced pressure: ^{13}C NMR (100 MHz, D_2O) δ 24.40, 24.85, 25.90, 25.99, 50.65, 66.97, 70.37, 70.78, 71.14, 96.32, 108.76, 109.60.

Synthesis of 6-Azido-6-deoxy-D-galactose. The deprotected azido galactose was synthesized as follows according to a procedure described previously.[18] 6-Azido-6-deoxy-1,2:3,4-diisopropylidene-D-galactose (0.50 g, 1.75 mmol) was stirred in 2.1 mL of 80% acetic acid at 70 °C for 16 h. After concentration of the solvent under reduced pressure, 10 mL of water was added to the residue and extracted four times with 10 mL of CH_2Cl_2. The aqueous phase was evaporated to afford 0.12 g (33% yield) of the deprotected azido galactose as a brown viscous oil: ^{13}C NMR (100 MHz, D_2O) δ 52.50, 52.64, 70.23, 70.39, 70.70, 71.00, 71.40, 73.53, 74.80, 75.04, 94.22, 98.70.

Synthesis of NDI-DS1. A *t*-BuOH/H_2O mixture (2:1, 3.0 mL) was added to *N*,*N*′-bis{[3-(3-propargyl)piperazin-1-yl]-propyl}naphthalene-1,4,5,8-tetracarboxylic acid diimide (NDI-1, 0.16 g, 0.10 mmol),[19] 6-azido-6-deoxy-D-galactose (0.12 g, 0.58 mmol), 1.0 M $CuSO_4$ (40 μL), 1.0 M sodium ascorbate (40 μL), and tris[(1-benzyl-1*H*-1,2,3-triazol-4-yl)methyl]amine (TBTA, 11 mg, 2.0 mmol) and stirred for 48 h at room temperature. NDI-DS1 was obtained as a yellow viscous oil and purified as follows. A peak at a retention time of 10 min (Figure 13S of the Supporting Information) was collected by reverse-phase high-performance liquid chromatography (HPLC) using an Inertsil ODS-3 column (inner diameter, 5 μm; size, 4.6 mm × 250 mm; GL Science Inc., Tokyo, Japan) in a gradient mode at a flow rate of 1.0 mL min^{-1}, where the MeOH concentration was changed linearly from 20 to 100% in water containing 0.1% trifluoroacetic acid over 40 min at 40 °C and subsequently freeze-dried: MALDI-TOF-MS [matrix, 2,5-dihydroxybenzoic acid (DHBA) (Figure 14S of the Supporting Information)] *m*/*z* [M + H] = 1205.16 (theoretical value, $C_{56}H_{78}N_{14}O_{16}$ + H^+ = 1204.31); ^{1}H NMR [500 MHz, D_2O (Figure 15S of the Supporting Information)] δ 2.14 (4.3, t, *J* = 7.5 Hz), 2.50 (4.2,

dx.doi.org/10.1021/bc500263b | *Bioconjugate Chem.* 2014, 25, 1547−1555

t, J = 7.0 Hz), 3.05−3.14 (15.2, m), 3.39 (5.2, t, J = 4.0 Hz), 3.50−3.80 (8.6, m), 3.86 (1.1, d, J = 2.0 Hz), 3.95 (0.68, d, J = 4.0 Hz), 4.14 (3.9, t, J = 7.0 Hz), 4.31 (0.7, d, J = 4.0 Hz), 4.48 (1.1, d, J = 2.0 Hz), 4.5−4.65 (3.8, m), 5.06 (0.72, d, J = 4.0 Hz), 7.80 (2.0, s), 8.47 (4.0, s).

Synthesis of NDI-DS2. A t-BuOH/H_2O mixture (2:1, 3.0 mL) was added to N,N'-bis[3-(3-propargyl)-methylaminopropyl]naphthalene-1,4,5,8-tetracarboxylic acid diimide (0.03 g, 0.062 mmol),[20] 6-azido-6-deoxy-D-galactose (25 mg, 0.12 mmol), 1.0 M $CuSO_4$ (25 μL), 1 M sodium ascorbate (25 μL), and TBTA (0.66 mg, 1.2 μmol) and stirred for 21 h at room temperature. NDI-DS2 was obtained as a yellow viscous oil and purified as follows. A peak at a retention time of 20 min (Figure 16S of the Supporting Information) was collected by reverse-phase HPLC using an Inertsil ODS-3 column (inner diameter, 5 μm; size, 4.6 mm × 250 mm; GL Science Inc.) in a gradient mode at a flow rate of 1.0 mL min^{-1}, where the concentration of MeOH was changed linearly from 10 to 100% in water containing 0.1% trifluoroacetic acid over 30 min at 40 °C and subsequently freeze-dried: MALDI-TOF-MS [matrix, DHBA (Figure 17S of the Supporting Information)] m/z $[M + H]^+$ = 896.36 (theoretical value, $C_{56}H_{78}N_{14}O_{16}$ + H^+ = 896.0); ^1H NMR [400 MHz, $CDCl_3$, TMS (Figure 18S of the Supporting Information)] δ 2.81 (6.2, s), 3.24 (1.6, m), 3.37 (1.9, m), 3.47 (1.0, d, J = 3.0 Hz), 3.49 (1.0, d, J = 3.0 Hz), 3.67 (1.5, d, J = 2.0 Hz), 3.90 (0.91, d, J = 5.0 Hz), 3.97 (1.1, d, J = 5.0 Hz), 4.12 (4.11, m), 4.24 (1.7, m), 4.44−4.71 (5.1, m), 5.02 (0.7, s), 8.16 (s, 1.0), 8.51 (3.37, s).

Apparatus. The mass spectra (MS) were recorded using a VoyagerTM Linear-SA (PerSeptive Biosystems, Foster City, CA) by the time-of-flight mode with α-cyano-4-hydroxycinnamic acid as the matrix. The ^1H and ^{13}C NMR spectra were recorded using a Jeol JNM-A500 spectrometer operating at 400 and 100 MHz for ^1H and ^{13}C, respectively, with tetramethylsilane (TMS) as the internal standard. The circular dichroism (CD) spectra were recorded over the range of 220−550 nm using a Jasco J820 spectropolarimeter (Jasco Inc., Tokyo, Japan) under the following conditions: response, 2 s; sensitivity, 100 mdeg; speed, 20 nm min^{-1}; resolution, 0.1 nm; bandwidth, 2.0 nm; cumulated number, four times; measuring temperature, 25 °C. The electronic absorption spectra were recorded using a Hitachi 3300 spectrophotometer equipped with an SPR 10 temperature controller under the following conditions: slit width, 5 nm; speed, 600 nm min^{-1}. The kinetic experiments were performed using an SF-61 DX2 double-mixing stopped-flow system (Hi-Tech Scientific Inc.) equipped with a temperature controller (Lauda RE206). The single-wavelength kinetic records of absorbance versus time were recorded. The AFM images were recorded using a PicoSPM instrument (Molecular Imaging Inc.). The TEM and EDS measurements were recorded using a H-9000NAR microscope (Hitachi).

Measurement of CD Spectra. The CD spectra of 0.08 mM-bp CT-DNA were measured in the presence of 0, 3.3, 10, 20, or 32 μM NDI-DS1 or NDI-DS2 in 10 mM MES (pH 6.25) and 1.0 mM EDTA containing 100 mM NaCl.

Topoisomerase I Assay. The topoisomerase I assay was conducted according to a procedure described previously.[21] A mixture of 35 mM Tris-HCl (pH 8.0), 72 mM KCl, 5.0 mM $MgCl_2$, 5.0 mM DTT, 5.0 mM spermidine, 0.01% BSA, 0.5 μg/μL M13 or pBR322, and 0.25 unit/μL topoisomerase I was incubated in the presence of varied amounts of NDI-DS1 or NDI-DS2 (0−20 μM) at 37 °C for 2 h. After the addition of 100 μL of 1× TE buffer [10 mM Tris-HCl and 1 mM EDTA (pH 7.0)], 2.0 μL of 10% sodium dodecyl sulfate (SDS), and 0.5 μL of 20 ng/μL proteinase K, the mixture was incubated at 37 °C for 15 min. A 1:1 phenol/chloroform mixture (100 μL) was added, vortexed, and centrifuged, and the aqueous phase was collected. This operation was repeated five times. The aqueous solution was washed five times with 100 μL of a 24:1 chloroform/isoamyl alcohol mixture.

Gel Electrophoresis. The obtained pBR322 solution (12 μL) from the topoisomerase I assay containing 1× loading buffer was applied to a sample comb of a 1.0% agarose gel and electrophiles using Mupid-exU (Advance Co. Ltd.) with 18 V for 3.5 h. After the electrophoresis, the gel was stained with GelStar to photograph using a transilluminator.

Atomic Force Microscopy. According to the procedure of the topoisomerase I assay, 0.5 ng/μL M13 DNA was treated with 0.25 unit/μL topoisomerase I in 10 mM HEPES (pH 6.15) and 10 mM $MgCl_2$ in the presence of 0.5, 1.0, 2.0, or 5.0 μM NDI-DS1, and 50 μL of the obtained solution was placed on a cleaved mica plate and kept for 30 min. After samples had been washed four times with Milli-Q water (50 μL), AFM images of obtained plates were measured after dried in a desiccator overnight.

Scatchard Analysis Using UV−Vis Measurement. The UV−vis spectra of 5.0 μM NDI-DS1 or NDI-DS2 in 10 mM MES (pH 6.25) and 1.0 mM EDTA containing 100 mM NaCl were measured after we had added the required amount of CT-DNA and waited for 1 min at 25 °C. The Scatchard analysis was conducted by analyzing the change in the spectra at 384 nm, the wavelength at which the absorption of NDI derivatives is the largest and is expressed by eq 1:[13]

$$r/\mathrm{LF} = K(1 - nr)\{(1 - nr)/[1 - (n - 1)r]\}^{n-1} \quad (1)$$

where r (saturation fraction), LF (free NDI-DS concentration), n (sitting number), and K are the amount of bound ligand per DNA base pair, the amount of unbound ligand, the number of DNA base pairs covered by the ligand, and the binding constant, respectively.

Kinetic Analysis Using the Stopped-Flow Method. The kinetic analysis was conducted according to a procedure described previously.[13] The single absorbance at 384 nm versus time was recorded in 10 mM MES buffer (pH 6.25) containing 1.0 mM EDTA and 100 mM NaCl at 30 °C. When CT-DNA was present in a 5-fold excess (12.5, 17.5, 25, 37.5, or 50 μM-bp) over ligand (2.5, 3.5, 5, 7.5, or 10 μM, respectively), the rate constants for association of NDI-DS1 or NDI-DS2 with CT-DNA were obtained by fitting the exponential data of absorption change to the expression $A_1 \exp(k_1 t) + A_2 \exp(k_2 t)$, where A and k are the fractional amplitudes and rate constants, respectively, for a two-exponential fit. The intrinsic second-order association rate constant (k_a) and the dissociation rate constant (k_d) were obtained from the slope of the plot of the apparent association rate constant (k_{app}) versus the CT-DNA concentration according to the equation $k_{app} = k_a[\mathrm{DNA}] + k_d$.

The rate constant k_d for the dissociation of the ligand from CT-DNA was determined by SDS-driven dissociation measurements. Two types of solutions (1% SDS and CT-DNA−ligand complex) were mixed instantaneously using a piston, and the change in the absorption spectrum was measured soon after the mixing. Thus, when the CT-DNA−ligand complex was mixed with an SDS solution, free ligands were incorporated into the SDS micelles. Because this process is diffusion-controlled, the entire absorption change represents the k_d-dependent process,

and therefore, fitting of the kinetic trace by the two-exponential model provides the k_d values.

Silver Mirror Reaction of NDI-1, NDI-DS1, NDI-DS2, and Glucose. The silver mirror reaction was conducted according to a procedure described previously.[12] Solution A was prepared as follows. $AgNO_3$ (0.17 g, 1.0 mmol) was dissolved in Milli-Q water (1.0 mL) and added to 12% NH_4OH until a brown precipitate appeared, followed by the disappearance of the precipitate. Three solutions, 1−3, were prepared as 11 mM NDI-1, NDI-DS1, NDI-DS2, and glucose-containing 0.26 M NaOH. Solution A (2 μL) was spotted on three places on a glass plate, and solutions 1−3 (23 μL) were mixed with the spot of solution A. These spots were carefully observed.

Atomic Force Microscopy and Transmission Electron Microscopy of M13 DNA. The silver mirror reaction mixture was prepared by adding 0.1 M $AgNO_3$ in NH_4OH at pH 10.5. The Au reaction mixture was prepared as follows. KSCN (100 μL, 60 mg/mL) and $KAuCl_4$ (100 μL, 23 mg/mL) were mixed and centrifuged at 4000*g* and 25 °C for 1 min; the supernatant was removed, 800 μL of phosphate buffer (pH 5.5) added, 100 μL of hydroquinone (5.5 mg/mL) added, and the mixture delivered to the plate as drops. The solution (50 μL) containing linearized M13 DNA with *Eco*RI digestion (0.16 ng/μL) or λDNA (0.001 ng/μL) in 10 mM HEPES (pH 6.15) and 10 mM $MgCl_2$ in the presence of 0.4 or 2.3 μM NDI-DS1 or NDI-DS2 was placed on a cleaved mica plate and kept for 30 min. After being washed four times with Milli-Q (50 μL) water, the plate was dried in a desiccator overnight. The silver mirror reaction mixture (0.1 M, 50 μL) was added to this plate, which was kept in a dark room for 5 h, and the plate was washed four times with 50 μL of Milli-Q water (total, 200 μL). The Au reaction mixture (50 μL) was also added to the plate, and the plate was kept for 30 s and dried in a dark room overnight. The AFM measurement was taken in a tapping mode at a scan rate of 2 GHz.

An elastic carbon support membrane-immobilized Au100 mesh (Okenshoji Co., Ltd., Tokyo, Japan) was used in the TEM measurements. A mixture of 1.5 nM NDI-DS and 0.001 ng/μL M13 was placed on the membrane and dried overnight in a desiccator. After 50 μL silver mirror reaction mixture was placed on the membrane and kept for 5 h, the membrane was washed twice with 5 μL of Milli-Q water. TEM measurements were taken after the samples had been dried overnight in a desiccator.

■ ASSOCIATED CONTENT

Ⓢ Supporting Information

Experimental procedure (SPR measurement) and Figures 1S−14S (^{1}H NMR spectra, HPLC data, MALDI-TOF-MS data, UV−vis spectra, CD spectra, SPR spectra, viscometric titration, topoisomerase I assay results, and AFM images). This material is available free of charge via the Internet at http://pubs.acs.org.

■ AUTHOR INFORMATION

Corresponding Author

*Phone: +81-93-884 3322. Fax: +81-93-884 3322. E-mail: shige@che.kyutech.ac.jp.

Notes

The authors declare no competing financial interest.

■ ACKNOWLEDGMENTS

This work was supported in part by Grants-in-Aid for Scientific Research from the Ministry of Education, Science, Sports and Culture, Japan.

■ REFERENCES

(1) De Volder, M. F., Tawfick, S. H., Baughman, R. H., and Hart, A. J. (2013) Carbon nanotubes: Present and future commercial applications. *Science 339*, 535−539.
(2) Wang, K., Wu, H., Meng, Y., and Wei, Z. (2014) Conducting polymer nanowire arrays for high performance supercapacitors. *Small 10*, 14−31.
(3) Chen, Y. J., Hsu, J. H., and Lin, H. N. (2005) Fabrication of metal nanowires by atomic force microscopy nanoscratching and lift-off process. *Nanotechnology 16*, 1112−1115.
(4) Pinheiro, A. V., Han, D., Shih, W. M., and Yan, H. (2011) Challenges and opportunities for structural DNA nanotechnology. *Nat. Nanotechnol. 6*, 763−773.
(5) Seeman, N. C. (1998) Nucleic acid nanostructures and topology. *Angew. Chem., Int. Ed. 37*, 3220−3238.
(6) Rothemund, P. W. (2006) Folding DNA to create nanoscale shapes and patterns. *Nature 440*, 297−302.
(7) Liu, D., Wang, M., Deng, Z., Walulu, R., and Mao, C. (2004) Tensegrity: Construction of rigid DNA triangles with flexible four-arm DNA junctions. *J. Am. Chem. Soc. 126*, 2324−2325.
(8) Gu, H., Chao, J., Xiao, S. J., and Seeman, N. C. (2009) Dynamic patterning programmed by DNA tiles captured on a DNA origami substrate. *Nat. Nanotechnol. 4*, 245−248.
(9) Han, D., Pal, S., Nangreave, J., Deng, Z., Liu, Y., and Yan, H. (2011) DNA origami with complex curvatures in three-dimensional space. *Science 332*, 342−346.
(10) Braun, E., Eichen, Y., Sivan, U., and Ben-Yoseph, G. (1998) DNA-templated assembly and electrode attachment of a conducting silver wire. *Nature 391*, 775−778.
(11) Patolsky, F., Weizmann, Y., Lioubashevski, O., and Willner, I. (2002) DNA and polylysine templated Au-nanoparticle nano-wires. *Angew. Chem., Int. Ed. 41*, 2323−2327.
(12) Fischler, M., Simon, U., Nir, H., Eichen, Y., Burley, G. A., Gierlich, J., Gramlich, P. M. E., and Carell, T. (2007) Formation of bimetallic Ag−Au nanowires by metallization of artificial DNA duplexes. *Small 3*, 1049−1055.
(13) Tanious, F. A., Yen, S. F., and Wilson, W. D. (1991) Kinetic and equilibrium analysis of a threading intercalation mode: DNA sequence and ion effects. *Biochemistry 30*, 1813−1819.
(14) Berge, T., Jenkins, N. S., Hopkirk, R. B., Waring, M. J., Edwardson, J. M., and Henderson, R. M. (2002) Structural perturbations in DNA caused by bis-intercalation of ditercalinium visualised by atomic force microscopy. *Nucleic Acids Res. 30*, 2980−2986.
(15) Richter, J., Seidel, R., Kirsch, R., Mertig, M., Pompe, W., Plaschke, J., and Schackert, H. K. (2000) Nanoscale palladium metallization of DNA. *Adv. Mater. 12*, 507−509.
(16) Davidson, M. W., Griggs, B. G., Boykin, D. W., and Wilson, W. D. (1977) Molecular structural effects involved in the interaction of quinolinemethanolamines with DNA. Implications for antimalarial action. *J. Med. Chem. 20*, 1117−1122.
(17) Morís-Varas, F., Qian, X. H., and Wong, C. H. (1996) Enzymatic/chemical synthesis and biological evaluation of seven-membered iminocyclitols. *J. Am. Chem. Soc. 118*, 7647−7652.
(18) Kong, D. C. M., and von Itzstein, M. (1997) The chemoenzymatic synthesis of 9-substituted 3,9-dideoxy-D-*glycero*-D-*galacto*-2-nonulosonic acids. *Carbohydr. Res. 305*, 323−329.
(19) Ohtsuka, K., Komizo, K., and Takenaka, S. (2010) Synthesis and DNA binding behavior of a naphthalene diimide derivative carrying two dicobalt hexacarbonyl complexes as an infrared DNA probe. *J. Organomet. Chem. 695*, 1281−1286.
(20) Watanabe, S., Sato, S., Ohtsuka, K., and Takenaka, S. (2011) Electrochemical DNA Analysis with a Supramolecular Assembly of

Naphthalene Diimide, Ferrocene, and β-Cyclodextrin. *Anal. Chem. 83*, 7290−7296.
(21) Webb, M. R., and Ebeler, S. E. (2003) A gel electrophoresis assay for the simultaneous determination of topoisomerase I inhibition and DNA intercalation. *Anal. Biochem. 321*, 22−30.

■ NOTE ADDED AFTER ASAP PUBLICATION

This paper was published ASAP on July 23, 2014, with errors in the TOC graphic, Abstract graphic, Figure 1, and Figure 2. The corrected version was reposted on July 28, 2014.